Binding of a Protein or a Small Polyelectrolyte onto Synthetic Vesicles

ARTICLE *in* LANGMUIR · FEBRUARY 2014

Impact Factor: 4.46 · DOI: 10.1021/la500199w · Source: PubMed

3 AUTHORS:

Fabiola Sciscione
Sapienza University of Rome
2 PUBLICATIONS **3** CITATIONS
SEE PROFILE

Carlotta Pucci
Sapienza University of Rome
12 PUBLICATIONS **27** CITATIONS
SEE PROFILE

Camillo La Mesa
Sapienza University of Rome
133 PUBLICATIONS **1,818** CITATIONS
SEE PROFILE

Langmuir
Msc: la500199w

The following graphic will be used for the TOC:

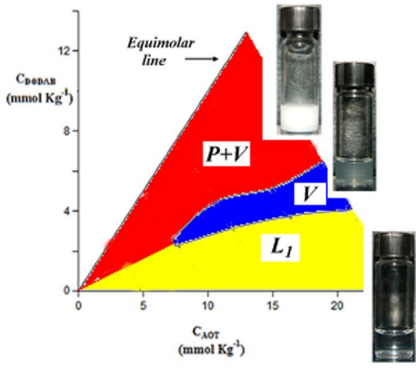

Langmuir

Article

pubs.acs.org/Langmuir

Binding of a Protein or a Small Polyelectrolyte onto Synthetic Vesicles

Fabiola Sciscione, Carlotta Pucci, and Camillo La Mesa*

Department of Chemistry, Cannizzaro Building, La Sapienza University, P.le A. Moro 5, I-00185 Rome, Italy

ABSTRACT: Catanionic vesicles were prepared by mixing nonstoichiometric amounts of sodium bis(2-ethylhexyl) sulfosuccinate and dioctyldimethylammonium bromide in water. Depending on the concentration and mole ratios between the surfactants, catanionic vesicular aggregates are formed. They have either negative or positive charges in excess and are endowed with significant thermodynamic and kinetic stability. Vesicle characterization was performed by dynamic light scattering and electrophoretic mobility. It was inferred that vesicle size scales in inverse proportion with its surface charge density and diverges as the latter quantity approaches zero and/or the mole ratio equals unity. Therefore, both variables are controlled by the anionic/cationic mole ratio. Small-angle X-ray scattering, in addition, indicates that vesicles are unilamellar. Selected anionic vesicular systems were reacted with poly-L-lysine hydrobromide or lysozyme. Polymer binding continues until complete neutralization of the negatively charged sites on the vesicles surface is attained, as inferred by electrophoretic mobility. Lipoplexes are formed as a result of significant electrostatic interactions between cationic polyelectrolytes and negatively charged vesicles.

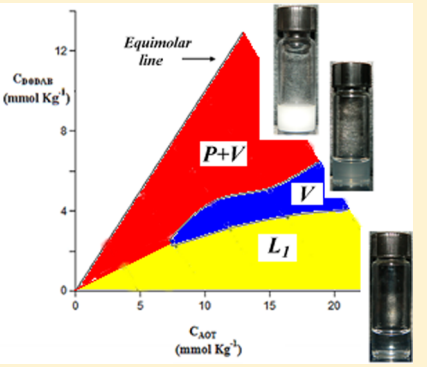

INTRODUCTION

The deep interest toward vesicular particles arises from the possible applications of such entities as structural and functional analogues of biological cells.[1−3] General consensus exists on their potentialities in biomedicine and ancillary technologies.[4,5] Studies reported so far focus on the friendly use of vesicles as carriers of diverse biopolymers, including nucleic acids.[6,7] The latter adsorb onto vesicles through electrostatic, hydrophobic, osmotic effects, and/or combinations thereof. The relative weight of each contribution depends on the medium, on the nature of the bilayer, and of the biopolymer as well. Because of electrostatic repulsions, free nucleic acid salts hardly cross membrane bilayers. Conversely, they easily adsorb onto positively charged vesicles. The process leads to the formation of [vesicle/nucleic acid] complexes, termed lipoplexes, which easily enter the cell trough fusion with its membrane, by pynocytosis or endocytosis. In words, the lipoplexes act as chaperones for the transfer across cell membranes. This is the reason why such biopolymer-based formulations are promising vectors for transfection technologies and/or gene therapy.

Crucial is the vectors' fate after the transfection procedures have been completed. In practical biomedical applications, the vesicular entities must be biodegradable and fully recyclable once the process is completed. For this to occur, the byproducts that are formed at the end of the above pathways must be nontoxic and fully compatible with the cell pool. The ones mentioned above are delicate items to face with and were the subject of dedicate research, intended to replace commercially available, but toxic, ionic surfactants with noncytotoxic ones. On this goal, amino acid−based or sugar-based species are the more promising chemicals considered today.[8,9]

Studies on transfection technologies mostly deal with lipid-based vesicles as carriers.[10] The above matrices, unfortunately, are thermodynamically and kinetically unstable, even though sonication, sterical stabilization,[11] pH, or added electrolytes slow down their coagulation. For the above reasons, biomedical investigations were progressively oriented toward stable vesicular systems, endowed with some features of the transfectors effectively operating in nature. Vesicles obtained by mixing oppositely charged surfactants, or lipids, in nonstoichiometric ratios deserved particular attention for the above reasons.[12,13] The processes leading to their formation are rendered possible by the combination of hydrophobic and electrostatic contributions. The resulting aggregates, termed catanionic, have net charge ≠0 and are characterized by a substantial thermodynamic stability. They can be made by one or more concentric bilayers; it is possible getting bilayered ones by raising the working temperature, and, then, turning back to the original conditions.[14] Such layered structures adsorb biopolymers; they also encapsulate drugs, sterols, and anti-biotics.[15] Biomedical applications of vesicle-based formulations are thus at hand, provided their biocompatibility is known and the related cytotoxicity minimized.[16] Use of surfactant-based catanionic vesicles has noticeable advantages and suffers from some drawbacks. In particular, (1) commercially available ionic surfactants are pure and cheap, but may be toxic, (2) the catanionic vesicles they form are much less cytotoxic than the surfactants from which are made of,[17] (3) ad hoc synthetic procedures can be eventually engineered to get nontoxic

Received: January 16, 2014
Revised: February 19, 2014

dx.doi.org/10.1021/la500199w | *Langmuir* XXXX, XXX, XXX−XXX

surfactants, (4) in all cases mentioned above, catanionic vesicles are easily prepared upon mixing oppositely charged surface active species, (5) vesicles are endowed with a substantial thermodynamic and/or kinetic stability,[18] (6) they are tunable in size and surface charge density, when proper mole ratios are used, and (7) if the surfactants are mixed in stoichiometric amounts, the formation of neutral catanionic precipitates occurs.

Catanionic vesicles are versatile matrices, since their surface charge density and size are tuned by the cationic/anionic mole ratio, *R*, still keeping fixed the overall surfactant concentration. Once the region of existence of vesicles in the phase diagram is characterized, it is possible getting "ad hoc" entities that interact with proteins, polynucleotides, etc. The biopolymer adsorption efficiency depends on its own charge density and on that of the vesicles as well. It is possible, therefore, to modulate biopolymer binding by changing the anionic/cationic mole (charge) ratio, the medium pH, and/or ionic strength. These are the reasons justifying the characterization of vesicles formed by mixing oppositely charged surfactants or lipids.

Catanionic mixtures made of sodium bis(2-ethylhexyl) sulfosuccinate, AOT, didodecyldimethylammonium bromide, DDAB, and water were extensively characterized, among many others, by Caria and Khan.[19] DDAB, a double chain surfactant, has a strong antibacterial character and is quite toxic to cells. This is a rather serious drawback to face with when DDAB is eventually used in transfection technologies. Fortunately, its catanionic mixtures are much less toxic than the single components.[20] Other possibilities are at hand, namely, (i) using nontoxic surfactants or (ii) reducing their cytotoxicity by appropriate formulation procedures. It is well-known, on this regard, that short alkyl chains are less toxic and have better transfection efficiency compared to long chain ones.[21] To improve the biocompatibility of catanionic vesicles, therefore, we replaced DDAB with dioctyldimethylammonium bromide, DODAB, a short-chain homologue of the former.

Efforts were devoted to characterize the regions where the cationic, or anionic, species is in excess. We formerly investigated the partial phase diagram of the system AOT/DODAB/H_2O, when the cationic species was dominant; we also determined the binding efficiency of an anionic polyelectrolyte onto positively charged vesicles.[22]

It is hardly predictable "a priori" if the behavior of the AOT/DODAB system is symmetrical with respect to mole ratios, charge, and overall surfactant concentration. For such an eventuality to occur, the critical micellar concentrations, CMCs, of the respective surfactant species must be very close, and the same holds for the areas at interfaces. As a matter of fact, they differ of 1 order of magnitude (≈2.5 and 20 mmol kg^{-1} for AOT and DODAB, respectively). It is expected, therefore, that vesicles size and charge density are not symmetrical with respect to the cationic/anionic mole ratio.[23−25] To get complete results on the system under scrutiny, therefore, we report here the case when AOT is in excess. Each region in that part of the phase diagram was characterized in detail. From a thermodynamic viewpoint, the AOT/DODAB/H_2O system is pseudoternary, since metathesis occurs upon mixing the components, with subsequent counterion exchange and formation of NaBr. As indicated in the following, this fact has some advantages.

In this contribution, we also checked whether electrostatic effects control the binding efficiency. This is the reason why species having the same nominal number of charges were compared. In spontaneous pH conditions, LYSO, lysozyme, has eight charges, as PLLHB, poly-L-lysine hydrobromide. Perhaps, the protein has different size and shape compared to the polypeptide, a much higher hydrodynamic volume, and a significantly lower charge density. The above considerations lead us to face with the inherent intricacies. The conformational changes of LYSO and PLLHBr depend on pH and on the state of charge of the vesicular entities onto which they adsorb. It is conceivable that surface adsorption and the resulting biopolymer conformation are mostly governed by electrostatic interactions. Excluded volume effects and subsequent repulsions between adjacent polyelectrolytes, presumably, may be significant only close to the surface saturation threshold. The above systems, therefore, represent good model systems to quantify the binding of polyelectrolytes onto oppositely charged vesicles.

The results presented here are justified by the need to characterize vesicle-based lipoplexes. The investigation was performed by dynamic light scattering (DLS) and ζ-potential. The above methods determined the average aggregates size and surface charge density, respectively. SAXS gave information on vesicle size and inner structure; in particular, it allowed to ascertain if bi- or multilayered vesicles are present. Ancillary techniques, such as optical absorbance, circular dichroism, CD, and ionic conductivity, supported the above findings. Combination of the results allows defining the molecular interactions that effectively take place when vesicles are titrated with polyelectrolytes. It is possible, thus, to account for the role of the polymer molecular details (i.e., mass, size, polar headgroup, charge, and conformation) in the interaction mechanisms. We determined the lipoplexes stability, evaluated the interaction modes, and draw some predictions on vesicles binding of small DNA and RNA sequences, which find extensive use in gene therapy.[24,25]

EXPERIMENTAL SECTION

Materials. Sodium bis(2-ethyhexyl)sulfosuccinate (AOT, Fluka) has nominal purity of 98% and was purified as in previous work.[29] Conductometric determination of its critical micellar concentration, CMC ≈ 2.5 mmol kg^{-1}, was a purity criterion. DODAB, of 98% nominal purity, was from TCI. It was dissolved in hot ethanol, filtered, and precipitated by cold acetone. The precipitate was dried overnight in an air oven at 70 °C. DODAB is hygroscopic and was stored over P_2O_5 until use. Surface tension and conductivity determined the CMC ≈ 20 mmol kg^{-1} [30,31] and its purity.

Poly-L-lysine hydrobromide (PLLHB, Sigma-Aldrich) was used as such. Its average molecular mass (≈2.2 kDa) was determined by intrinsic viscosity.[32] Chicken egg-white lysozyme (LYSO, Sigma-Aldrich) was dialyzed in 150 mmol kg^{-1} NaCl, recovered, dried, lyophilized, and kept over P_2O_5 until use. NaBr (Sigma-Aldrich) was dried at 150 °C and used as such. HBr and NaOH (Carlo Erba) were eventually added to adjust the pH of PLLHB-containing dispersions. Water was doubly distilled over alkaline $KMnO_4$ and bubbled by N_2 to minimize CO_2 uptake. At 25.00 °C, its ionic conductance is $<1 \times 10^{-7}$ Ω^{-1} cm^{-1}.

The catanionic mixtures were prepared by weighing the components in glass vials, which were flame-sealed and kept at 25 °C until macroscopic equilibrium was attained. The different phases that are formed were checked by inspection in white or polarized light, eventually with the aid of optical microscopy. Investigations were repeated until the macroscopic appearance of the samples remained constant. Subsequent DLS measurements determined the average aggregate size. In that case, care was taken to ascertain if vesicle size distributions changed upon aging.

Thereafter, the two polyelectrolytes were added to the vesicular dispersions on a weight percent basis. The characterization of

dx.doi.org/10.1021/la500199w | *Langmuir* XXXX, XXX, XXX−XXX

lipoplexes formed by each of the aforementioned polyelectrolytes and anionic-rich vesicles was made using the same procedures as indicated above.

Methods. *Optical Polarizing Microscopy.* An optical CETI-Laborlux Topic microscope operated in white or polarized light, and in conoscopy mode, at 25 °C. The samples were put on accurately cleaned slides and covered by a glass sheet. The sample thickness was modulated to optimize the image(s) quality. On this goal, thin Teflon spacers were inserted between the slide and the cover slide. Sometimes the dispersions contain large particles or exhibit optical anisotropy. In polarized light such multiphase dispersions may show maltese crosses, mosaic, and/or oily streaks textures.[33−35] It is possible, thus, to recognize the presence of liquid crystalline or solid phases.

Dynamic Light Scattering (DLS). Measurements were run by a Malvern Zeta Nanosizer, working at 632.8 nm in backscattering mode (173°), at 25.0 ± 0.1 °C. That configuration allows determining reliable particles sizes even in the presence of significant turbidity. The digital correlator analyzed the scattered light intensity fluctuations due to Brownian motions, $I(\vec{q},t)$, at times t and $(t + \tau)$, respectively. The measuring unit automatically transformed the NNLS decays into CONTIN ones. $G_2(\vec{q},t)$, the autocorrelation function, was determined according to

$$G_2(\vec{q}, t) = \frac{\langle I(\vec{q}, t)\cdot I(\vec{q}, t + \tau)\rangle}{\langle I(\vec{q})^2\rangle} \quad (1)$$

where $\vec{q}$ is the scattering vector, τ the delay time, and the brackets indicate a time average. $G_2(\vec{q},t)$ is related to the electromagnetic field autocorrelation function, $g_1(\vec{q},t)$, through the equation

$$G_2(\vec{q}, t) = A + B|g_1(\vec{q}, t)^2| \quad (2)$$

where A is the baseline and B depends on the aggregates. The $g_1(\vec{q},t)$ function was expanded through a cumulant analysis[36] to give

$$\ln[g_1(\tau)] = -\Gamma_1\tau + \left(\frac{\Gamma_2}{2}\right)\tau^2 \quad (3)$$

where Γ_1 is the first cumulant. That quantity gives the self-diffusion coefficient of the particles, D (in $cm^2\ s^{-1}$), related to their hydrodynamic radius through the Stokes−Einstein equation. Γ_2, conversely, is proportional to the polydispersity index, PdI. The latter quantity is close to 0.1 in case of vesicles; it increases when polyelectrolytes are added and reaches a maximum close to the charge neutralization threshold.

Electrophoretic Mobility. Measurements were run by a Laser-Doppler facility available in the DLS unit. It operates on cells equipped with gold-coated electrodes, at 25.0 ± 0.1 °C. From electrophoretic mobility values, μ, the ζ-potential, ζ (mV), was determined. In fact[37]

$$\zeta = \mu\left(\frac{4\pi\eta}{\varepsilon^\circ}\right) \quad (4)$$

where η is the solvent viscosity and ε° is its static dielectric permittivity. In eq 4, no restrictions is placed on the particle shape, save for the assumption that the radii of curvature of the surface are everywhere much greater than Debye's screening length, κ^{-1}.[38] Smoluchowski's approximation holds because the electrical double layer thickness surrounding vesicles, or lipoplexes, δ, is much lower than $D_H/2$.[39]

Small-Angle X-ray Scattering (SAXS). Measurements were run at ELETTRA SAXS beamline, Trieste (Italy). Data were recorded on a bidimensional plate detector, radially averaged, and corrected for the dark, empty capillary, and buffer contributions.[40] The investigated Q-range ($Q = 4\pi \sin\theta/\lambda$ where 2θ is the scattering angle and $\lambda = 1.54$ Å) was 0.09−3.0 nm^{-1}. Experiments were run at 25.0 ± 0.1 °C. The acquisition time was 4 min long.

Circular Dichroism and UV−vis Methods (CD and UV). A J-180 Jasco spectropolarimeter, equipped with a 450 W Xe lamp, was used. Measurements were performed at 25.0 ± 0.1 °C in the 190−250 nm λ range, using cells with path lengths between 0.010 and 0.10 cm. The conformational analysis was performed as in previous work.[39] UV−vis spectra were recorded by a Jasco-V550 spectrophotometer, at 25.0 ± 0.1 °C, using quartz cells with path lengths in the range 0.100−1.00 cm.

Ionic Conductivity. A 6425 Wayne-Kerr precision component analyzer, working at 1.00 kHz, was used. The cell containing the dispersion was located in an oil bath at 25.000 ± 0.003 °C. Addition of polyelectrolytes to the dispersions was performed by a weight buret. The individual readings were taken about 15 min after attainment of thermal equilibrium, under moderate and continuous stirring. That procedure avoids the sedimentation of the lipoplexes that are eventually formed.

RESULTS

Phase Diagram. Compared to AOT, the supramolecular association features of DODAB occur at quite high concentrations. In ternary systems, perhaps, the formation of mixed micelles and vesicles occurs at much lower concentrations than those pertinent to the pure surfactants.[41,42]

The partial phase diagram was investigated at an overall surfactant concentration ≤1.10 wt % (≈25 mmol kg^{-1}) at 25.0 °C. The vesicular region and multiphase areas were determined. Some samples present a bluish color and are optically isotropic; in cases like such vesicles have sizes in the 10^2 nm range. At concentrations between 2.0 and 3.0 mmol kg^{-1} and R ratios ≈1, the dispersions are turbid and large aggregates were observed by DLS. Large vesicles are unstable and form low-density catanionic fluids, hardly phase-separated by centrifugation. After application of high gravitational fields for a few hours, however, the mixtures reach the equilibrium conditions. Thereafter, the vesicular dispersions coexist with whitish precipitates.

It is not easy to characterize the dilute regimes in much detail, but when the overall surfactant content is ≥5 mmol kg^{-1}, the vesicular area is easily characterized (Figure 1). For [AOT/DODAB] mole ratios close to unity, the samples are milky; in that region, the vesicular dispersions coexist with a solid and form two-phases, indicated as Pr+Ve in Figure 2. The onset of precipitates was completed some days after preparation;

Figure 1. Turbidity of AOT−DODAB−H_2O mixtures, containing 15.0 mmol kg^{-1} of surfactant. The [AOT/DODAB] mole ratios are 1.53 (A), 3.02 (B), and 4.50 (C). The images refer to samples equilibrated at room temperature for more than 24 h.

dx.doi.org/10.1021/la500199w | Langmuir XXXX, XXX, XXX−XXX

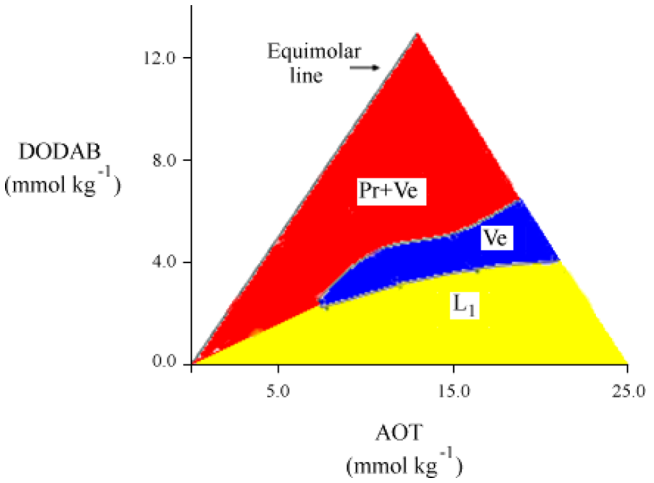

Figure 2. Anionic-rich region of the AOT/DODAB/H_2O system, at 25.0 °C. The concentrations of DODAB and AOT are in mmol kg^{-1}. The equimolar line, the vesicular region, Ve, the solution one, L_1, and the two phase vesicle-solid area, Pr+Ve, are indicated.

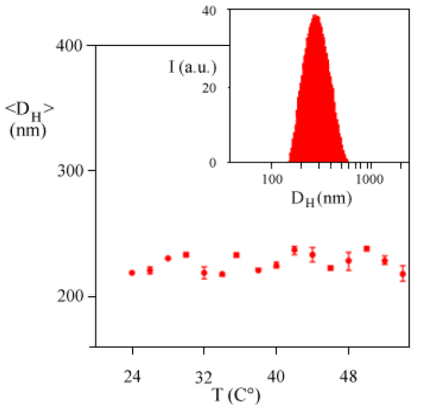

Figure 3. Dependence of the vesicle hydrodynamic diameter, D_H, nm, on temperature (°C), for a system of mole ratio R = 3.02 and overall surfactant content = 15.0 mmol kg^{-1}. In the inset is reported the intensity-based distribution function, I (au), vs D_H for the above sample, at 25.0 °C.

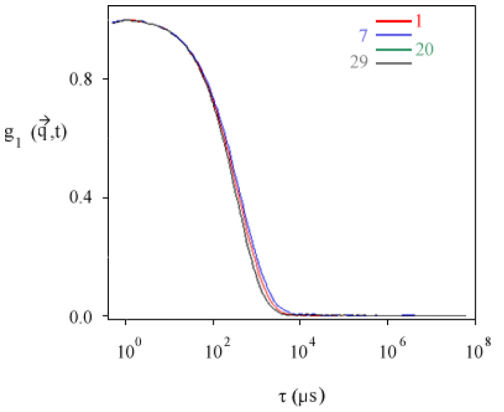

Figure 4. Plots of $g_1(\vec{q},t)$vs τ (μs), measured 1, 7, 20, and 29 days after preparation, at 25.0 °C. Data refer to the same system as in Figure 3.

therefore, the location of the phase boundaries was detected after long equilibration times. On increasing the [AOT/DODAB] mole ratios, the dispersion turbidity drastically decreases and the samples progressively become slightly opalescent. Finally, a bluish optically isotropic phase,[43] termed Ve, is attained. In that region vesicles dominate. For still higher mole ratios, the samples become transparent and optically isotropic. The latter region is a true micellar solution and is indicated as L_1 in the phase map.

Addition of LYSO, or PLLHB, increases the dispersions turbidity, until the polymer concentration reaches the charge neutralization threshold. Thereafter, the turbidity decreases and levels off. The ability of the two polymers to induce the formation of lipoplexes and their growth in size is qualitatively similar. Those containing lysozyme, anyhow, are much larger than the ones made of PLLHB. The molecular details underlying the formation and nature of the mentioned lipoplexes shall be outlined below.

Vesicles Size. To ensure the attainment of macroscopic equilibrium conditions, the systems were investigated 1 day after preparation at least. The average hydrodynamic diameter, D_H (nm), and ζ-potential, in mV, are reported in Figures 3 and 4, respectively. The kinetic and thermodynamic stability of catanionic vesicles is substantial: no changes in size occur upon aging or raising the temperature. The size distributions are monodisperse, with moderate PdI. When AOT is in strong excess, ζ-potentials are negative and increase in absolute values with mole ratios. Na^+ and Br^- ions are released from vesicles, as also inferred by conductivity. The observed effects scale with the overall surfactant concentration and R ratios.

When the [AOT/DODAB] mole ratio approaches unity, D_H values diverge. In the above conditions, ζ-potential tends to zero. This is because metathesis occurs, with subsequent ion exchange between AOT and DODAB. A nonancillary consequence of the process is a significant change in double layer thickness, δ, which is related to an increase in the bulk concentration of NaBr and depends on AOT/DODAB mole ratios. From a phenomenological viewpoint, the size of vesicular aggregates is proportional to the surface charge density, σ. This fact is consistent with former studies, where links between charge density and vesicle size were accounted for.[44]

The spontaneous radius of curvature for vesicular interfaces is such to minimize the electrostatic repulsions between adjacent, similarly charged, surfactant ions. Charging/discharging processes induce significant and regular changes in σ and in the aggregate size. At the charge neutralization, planar uncharged bilayers are formed and precipitation of a not soluble solid occurs. The above behavior is consistent with the "packing constraint theory"[45,46] and can be also generalized by the so-called "R theory", proposed by Winsor for the spontaneous curvature of fluid interfaces.[47] This is because the effective area occupied by oppositely charged species lying on the aggregate surface, A, is substantially lower than the sum of individual ones. In addition, the effective volume of hydrophobic moieties may change. At the charge neutralization threshold, therefore, the packing parameter, P (= V/AL, where the latter is the alkyl chain length), approaches unity. When the ratio of [AOT/DODAB] in mixtures is different from 1, vesicles or micelles (that occur when R is very high or very low) do form. The packing constraint hypothesis is consistent with DLS measurements performed on the anionic-rich side of the phase diagram (Figure 5).

According to the packing constraint theory, it is expected that size and shape transitions are concomitant to a series of

dx.doi.org/10.1021/la500199w | Langmuir XXXX, XXX, XXX–XXX

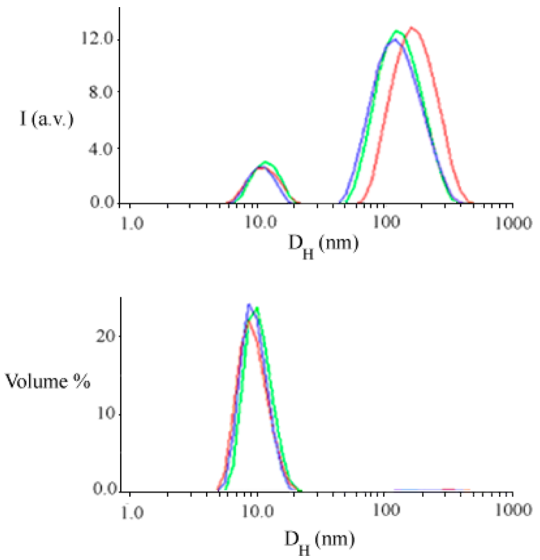

Figure 5. Intensity (top) and volume % (bottom) vs D_H plots for 15.0 mmol kg^{-1} AOT−DODAB systems of R ratios equal to 4.0 (red), 6 (green), and 10 (blue color), at 25.0 °C.

intermediate steps: i.e., spherical → anisometric → swollen micelles → vesicles. We noticed that vesicles and micelles coexist in part of the phase diagram and found that the relative amounts of the two organization states depend on R. In the experimental conditions depicted in Figure 5, the number density of micelles is much higher than that pertinent to vesicles. It must be pointed out that the lower limit of existence of the vesicular region is the point at which the presence of small micelles, inferred by intensity vs D_H plots, is negligible. Such empirical definition is, actually, the only way to define micelle−vesicle transitions. It must be also stressed that the phase boundaries obtained by DLS plots are very close to the appearance of a bluish color.

SAXS data (Figure 6) give information on size and inner vesicle structure.[48] $I(\vec{q})$ vs $\vec{q}$ plots indicate the absence of Bragg

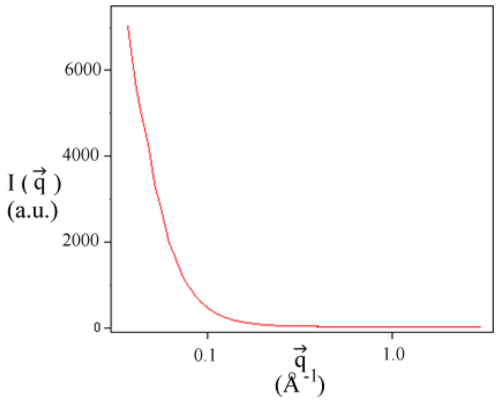

Figure 6. $I(\vec{q})$ vs $\vec{q}$ SAXS profile for a 15.0 mmol kg^{-1} AOT/DODAB mixture of R ratio = 3.5, at 25.0 °C.

peaks typical of layered structures; accordingly, vesicles are presumably endowed with a unilamellar character. This is, in our opinion, a clear-cut indication on the absence of multilayered entities. For physical consistency we assume it is a bilayer. The above hypothesis finds support from comparison with studies on similar catanionic systems. The transitions from multi- to bilayers are concomitant to the disappearance of the lamellar repetition peak (whose intensity is proportional to the number of bilayers).[14] No such changes have been observed in the present system. The determination of a single bilayer state is hardly detected in the present Q-range. Given the supposed constancy of the bilayered state, vesicles are very presumably more stable than multilamellar ones[49,50] and remain as such for indefinitely long times.

The interaction potential among vesicles, accordingly, is concomitant to the presence of a secondary minimum, which vanishes when the double layer thickness reduces. In fact, coagulation is observed when the concentration of free electrolyte increases, as observed close to the two-phase threshold in Figure 2. In that region Ostwald ripening is possible:[51] in such an eventuality, vesicles merge or nucleate into large ones, until phase separation takes place.

Interactions with PLLHB and LYSO. To quantify the interactions with polymers, we choose vesicular samples with optimal performances in terms of size, charge, and thermodynamic stability. All are endowed with a bilayer character and are located in the central part of the Ve region. The properties of vesicles used to experience polymer binding are reported in Table 1.

Table 1. Surfactant Concentration, C_{tot} (mmol kg^{-1}), [AOT/DODAB] Mole Ratio, R, Average Vesicle Hydrodynamic Diameter, D_H (nm), and ζ-Potential (mV) for Selected Vesicular Systems, at 25.0 °C

C_{tot} (mmol kg^{-1})	R ratio	D_H (nm)	ζ-potential (mV)
15.03	3.02	230 ± 6	−84 ± 4
20.02	3.51	212 ± 4	−82 ± 2
24.98	3.99	253 ± 3	−88 ± 4

ζ-Potential measurements performed on the above systems determined how addition of polyelectrolytes affects the vesicle surface charge density. Data in Figure 7 were normalized for the maximum number of charges in excess, z. In spontaneous pH

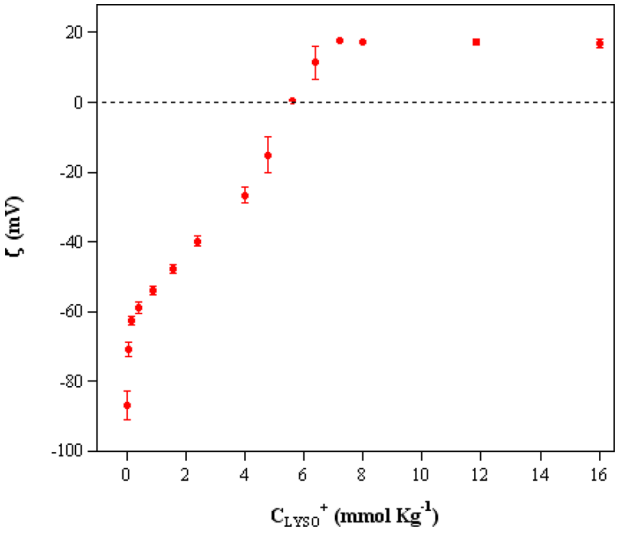

Figure 7. Dependence of ζ-potential (in mV) on the number of charges pertinent to LYSO, z (mmol kg^{-1}), at 25.0 °C; the value of z is 8. The vesicle concentration is 15.0 mmol kg^{-1} and the [AOT/DODAB] mole ratio is 3.02.The dotted line represents the charge inversion point. Bars indicate the errors.

dx.doi.org/10.1021/la500199w | Langmuir XXXX, XXX, XXX−XXX

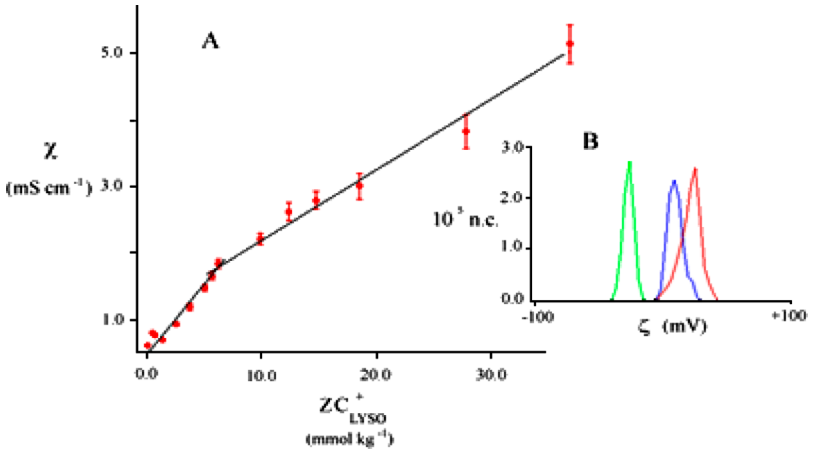

Figure 8. (A) Ionic conductivity, χ (mS cm^{-1}), of a 15.0 mmol kg^{-1} and 3.02 [AOT/DODAB] ratio vesicular dispersion titrated with PLLHB, at 25.00 °C. Data are reported as concentration C_{PPLHB}^{+} (mmol kg^{-1}) times the number of nominal charges, Z. (B) Population density, in number of counts (10^5 nc), vs ζ-potential (mV), for 2.5 (green), 5.9 (blue), and 9.9 (cyan) charge ratios between PLLHB and vesicles.

conditions lysozyme has 8 such charges,[52] and the same holds for PLLHB. For simplicity, the effective charge and counterion condensation thereon are not considered. Addition of LYSO, or PLLHB, results in a significant decrease in $|\zeta|$.

The point of zero charge is very nearly the same in the two cases. According to Figures 7 and 9, the polyelectrolytes adsorb onto vesicles, progressively reducing their surface charges. At $5.0 \leq zC_{LYSO}^{+} \geq 6.0$ mmol kg^{-1}, for instance, ζ-potentials approach zero and charge neutralization occurs.

The isoelectric point of LYSO-based lipoplexes is centered in that region. Further addition of LYSO imply the attainment of ζ-potentials pertinent to the free protein, $\approx$+17.3 $\pm$ 0.2 mV. Similar conclusions apply to PLLHB.

In both cases a deformable association colloid, the vesicle, is titrated with an intrinsic one. The systems undergo to charge inversion phenomena.[53] Polymers in excess are freely moving in the dispersion, as inferred by ionic conductivity on LYSO (Figure 8). In that region partial redissolution of precipitates was observed. In addition to charge neutralization, changes in size and shape occur. Biopolymer binding onto vesicles occurs through hydrophobic,[54] electrostatic interactions,[55] or a combination thereof.[56] In the first case, the hydrophobic parts of the biomacromolecules are located in the vesicle bilayer and form pores with sizes comparable to their cross section.[57] Purely electrostatic interactions, conversely, are peculiar to globular proteins. In that case, surface adsorption is favored compared to insertion in the bilayers until a peculiar concentration threshold is attained.[57] In the present systems the electrostatic interactions could be dominant. Protein insertion into bilayers, in fact, implies significant modifications in the vesicle structure, with subsequent changes in size. DLS showed that size changes occur; therefore, both hydrophobic and electrostatic contributions could be significant.

In such an eventuality, changes in polyelectrolyte conformation should be observed. Support to the latter hypothesis may come from CD. Unfortunately, conformational changes of the polyelectrolytes could not be detected with the required accuracy. In fact, AOT is a molecule with three stereogenic centers. The partial overlapping of signals due to its chiral moieties with those pertinent to polyelectrolytes, which adsorb in the same λ range, does not allow to assign univocally the spectral changes. Therefore, the hypothesis of hydrophobic interactions cannot be univocally supported from CD.

ζ-Potentials are related to the surface charge density of colloid objects, σ, through the relation

$$\sigma\tau = \frac{\varepsilon_r \varepsilon^\circ \zeta}{4\pi} \quad (5)$$

where ε° is the dielectric permittivity in vacuum, ε_r that of the dispersing fluid, and τ depends on the ionic strength of the medium through Debye's equation. Both τ and, to a lesser extent, ε_r depend on R.

Some authors replaced Smoluchowsky's equation, eq 5, with Ohshima's one. A 2/3 constant relates the two. Ohshima's relation applies to surfaces onto which polymers are adsorbed; therefore, the resulting surface is considered "soft". Both Ohshima's and eq 5 refer to particles with D/δ ratios $\gg$1 and significantly differ from Debye's one (which holds when $D/\delta \approx$ 1). In the case of noncoated vesicles, Smolochowski's relation is to be preferred, since no polymer is adsorbed and the vesicle surface is smooth. Corrections based on Ohshima, thus, should be made only in case of polymer-coated entities.[58−60] Using two equations for different regions in the same system, therefore, can be cumbersome, since it is not possible defining a reference value.

According to eq 5, ζ-potentials are proportional to an electric moment per unit area and depend on the surface charge density and the double layer thickness as well. Provided the latter quantity is known with due accuracy, it is possible getting σ as a function of C_{Polym} and to calculate changes in surface coverage with composition. Estimates based on the above assumptions were made in the case of PLLHB (Figure 9). Plots were corrected for the double layer thickness. It is evident that they are compatible with monolayer adsorption processes, since no discontinuities in σ values were observed above the charge neutralization threshold.

In terms of charge titration, there is substantial agreement between data relative to LYSO and those pertinent to PLLHB. The point of zero charge inferred by σ and ζ-potential plots (Figures 7 and 9) is nearly the same. This is an evidence in favor of the electrostatic nature of the interaction. Recall that the two polyelectrolytes have the same nominal charge. Conductometric titrations (Figure 8) support the above statements. The intersection point between the straight lines in the plot is the value above which ionic mobility is due to free PLLHB, or LYSO, in the presence of free NaBr. In Figure 8 are

dx.doi.org/10.1021/la500199w | Langmuir XXXX, XXX, XXX−XXX

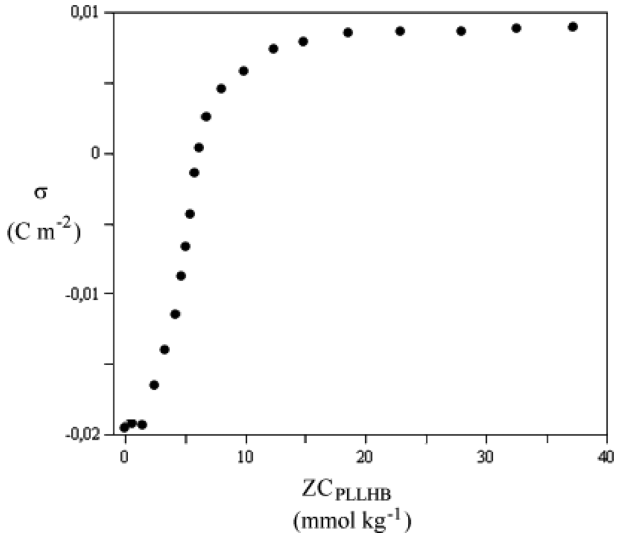

Figure 9. Surface charge density of lipoplexes, σ (C m^{-2}), vs the concentration of PLLHB (mmol kg^{-1}), times the number of nominal charges, Z, at 25.0 °C. Data refer to 15.0 mmol kg^{-1} of surfactant and an [AOT/DODAB] ratio = 3.02.

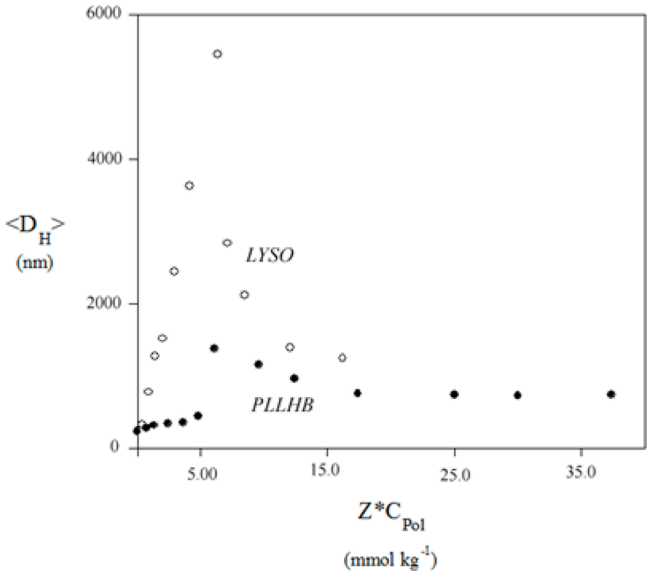

Figure 10. Lipoplexes size, D_H (nm), vs the polyelectrolyte concentration (mmol kg^{-1}) multiplied by the maximum number of charges, Z, at 25.0 °C. Vesicles contain 15.0 mmol kg^{-1} of surfactant, and the [AOT/DODAB] ratio is 3.02. The full line indicates the surface charge neutralization threshold.

also reported the distribution functions relative to the electrophoretic mobility, μ, of lipoplexes. From the plot it results that the behavior is controlled by the vesicle/titrant charge ratio; it approaches zero when that ratio is close to unity and shifts to positive values when the titrant is in excess. This is a strong evidence of the essentially electrostatic nature of the interaction.

Addition of PLLHB, or LYSO, to vesicular dispersions implies formation of lipoplexes, with growth and nucleation into large clusters. The maximum size of lipoplexes is attained at nearly the same nominal charge, as expected in case of purely electrostatic interactions. It is possible that the polymers act as linkers among different vesicles. In such an eventuality, the polymer size and net charge should be relevant in bridging the lipoplexes. If the hypothesis suits, LYSO-based lipoplexes would give rise to larger objects compared to those formed by PLLHB. Comparison of data (Figure 10) supports the above hypothesis. In fact, LYSO-based lipoplexes are significantly larger compared to those met in PLLHB-containing ones. It is conceivable that the relatively large hydrodynamic volume of LYSO has a key role in clustering activity. The protein has a volume nearly 2 times higher than PLLLHB. Notwithstanding the same nominal charge, LYSO has a much lower surface charge density and a substantially higher volume than PLLHB. Presumably, it is more easily inserted between adjacent vesicles, in such a way to minimize the reciprocal electrostatic repulsions when they are bound to the same polymer.

Calculations based on the molecular features of the two species indicate that the protein has a surface charge density 3 times lower than PLLHB (if the latter is considered an equivalent sphere), when its mass is about 8 times higher. On such grounds, the insertion of LYSO among two adjacent vesicles reduces their repulsive interaction potential and favors nucleation much more significantly than PLLHB. This is a plausible explanation for the growth in lipoplexes size observed when LYSO acts as a titrant.

Those mentioned above are rather obvious consequences of the molecular details inherent to the two biopolymers, which do not allow to modulate the effect on purely electrostatic interactions. Dobrynin developed a theory on the binding of linear polyelectrolytes onto charged surfaces. It refers to the binding onto flat unspecified surfaces and/or onto large spherical charged particles.[61−65] In the model the long-range nature of polyampholyte adsorption leads to the formation of an adsorbed layer much thicker than the size of individual chains. The regimes proposed in the theory are defined as pole, fence, and pancake, respectively.[61] In the former case it is supposed that the polyelectrolyte orientation around surfaces is similar to long facing outward dipoles. The second assumes that different parts of the polymer chain(s) are oriented parallel and antiparallel each other. The pancake one, finally, implies the presence of several binding occupied by the same polymer, with each junction separated from the other by a chain. At present, there is no direct experimental support to the validity of the theory. Surely, neither ζ-potential nor DLS allows discriminating the different binding modes that were proposed. We are personally convinced that the above theoretical hypotheses could be checked by dielectric relaxation, provided the different polyelectrolyte orientations are effectively as indicated in ref 61.

The pole model could satisfactorily apply to PLLHB, but it is hardly compatible with the protein, which is surely in a nonlinear configuration. Modeling the behavior of LYSO on such grounds is much more cumbersome than current hypotheses valid for linear polyelectrolytes. Another point in Dobrynin's theory is in clear disagreement with the present findings. According to Figure 10, the lipoplexes size steeply decreases at concentrations well above the surface saturation threshold. That behavior is hardly reconciled with theoretical predictions; in fact, the results are contradictory with respect to the model. That is, the field generated by the core particles is not strong enough to ensure layer-by-layer adsorption. Either it is possible that osmotic effects favor water uptake and desorption of the polymers from the lipoplex surfaces.

According to ζ-potential data, both polyelectrolytes neutralize nearly the same number of charges on the vesicle surface. For an [AOT/DODAB] R ratio = 3.02 and an overall

dx.doi.org/10.1021/la500199w | Langmuir XXXX, XXX, XXX−XXX

surfactant content of 15.0 mmol kg^{-1}, for instance, the maximum number of negative charges that are titrated is around 7.5 mmol kg^{-1}. About 80% of them are effectively neutralized, irrespective of whether PLLHB or LYSO is used. It is possible that more complex molecular architectures do not have the same performances as titrants than those mentioned above.

Excluded volume effects do not allow the onset of further binding stages onto the vesicle surface. Therefore, monolayer binding is expected to occur. This is in line with the adsorption of nearly stoichiometric amounts of polyelectrolytes onto the vesicle surface. It is assumed on such grounds that the significant increase in the lipoplexes size is related to a substantial clustering rather than to a progressive growth. We are confident that the best result in transfection efficiency are met at concentrations close to the saturation thresholds in Figures 7, 9, and 10. In such cases, the lipoplexes have moderate sizes and bear, in the same time, the due amounts of charges, which ensure a substantial binding efficiency onto vesicles.

■ CONCLUSIONS

Both PLLHB and LYSO strongly interact with catanionic vesicles; the process is essentially driven by electrostatic interactions. According to experimental evidence, a monolayer vesicle coverage occurs for concentrations equal to or slightly lower than those pertinent to charge neutralization. The size of lipoplexes is clearly modulated by the molecular structure of the polyelectrolytes. From a functional point of view, the complexes made by linear polypeptides are relatively smaller and, presumably, more reliable for binding onto cells than those made of LYSO.

Taking into account what reported here, it is expected that small DNA and/or RNA fragments behave similarly, when mixed with due amounts of oppositely charged vesicular entities. In cases when the electrostatic interactions are largely dominant with respect to others, we are confident that a close behavior to that reported here should be observed. DNA fragments, in particular, are relatively rigid and could safely interact with vesicles according to the same mechanisms as the ones depicted here for PLLHB. RNA fragments, conversely, are more easily deformed and are also endowed with a substantial hydrophobic character, ascribed to the presence of flexible chains with strong amphipatic character. Its binding, therefore, should be substantially different from the one depicted here.

It is indicated here that a substantial capability of modulation of lipoplexes properties is possible by choosing polyelectrolytes differing in size, charge, and molecular details. Therefore, ad hoc formulations are made possible by choosing the appropriate vesicular systems and components in such a way to have particles suitable for effective transfection technologies. The engineering part of this work is actually open to new and exciting routes. It is also required, on that purpose, to investigate the effective cytotoxicity of lipoplexes toward model cellular systems.

■ AUTHOR INFORMATION

Corresponding Author

*E-mail: camillo.lamesa@uniroma1.it (C.L.M.).

Notes

The authors declare no competing financial interest.

■ ACKNOWLEDGMENTS

This work was financed by "La Sapienza" University, Rome (IT), through a strategic project. It is partly based on the Ph.D. dissertation by C.P. It is also supported by the master thesis work of A.B. and F.S. Thanks to R. C. Zumpano and S. Zinkowskij (Masters in Chemistry, La Sapienza) for experimental support. Thanks to G. Risuleo (Dept. of Biology & Biotechnology, La Sapienza), A. Bonincontro (Dept. of Physics, La Sapienza), and A. Scipioni (Dept. of Chemistry, La Sapienza) for stimulating discussions during the manuscript preparation.

■ REFERENCES

(1) Soussan, E.; Cassel, S.; Blanzat, M.; Rico-Lattes, I. Drug delivery by soft matter: matrix and vesicular carriers. *Angew. Chem., Int. Ed.* **2009**, *48*, 274−288.

(2) Barenholz, Y.; Peer, D. Liposomes, lipid biophysics, and sphingolipid research: from basic to translation research. *Chem. Phys. Lipids* **2012**, *165*, 363−364.

(3) Jiang, Y.; Li, F.; Luan, Y.; Cao, W.; Ji, X.; Zhao, L.; Zhang, L.; Li, Z. Formation of drug/surfactant catanionic vesicles and their application in sustained drug release. *Int. J. Pharm.* **2012**, *436*, 806−814.

(4) Bhattacharya, S.; De, S.; Subramanianm, M. Synthesis and vesicle formation of hybrid bolaphile/ amphiphile ion pairs. Evidence of membrane property modulation by molecular design. *J. Org. Chem.* **1998**, *63*, 7640−7651.

(5) Kim, S.-H.; Kim, K.-S.; Lee, S.-R.; Kim, E.; Kim, M.-S.; Lee, E.-Y.; Gho, Y. S.; Kim, J.-W.; Bishop, R. E.; Chang, K.-T. Structural modifications of outer membrane vesicles to refine them as vaccine delivery vehicles. *Biochim. Biophys. Acta, Biomembr.* **2009**, *1788*, 2150−2159.

(6) Bonincontro, A.; La Mesa, C.; Proietti, C.; Risuleo, G. A biophysical investigation on the binding and controlled DNA release in a cetyltrimethylammonium bromide-sodium octyl sulfate catanionic vesicle system. *Biomacromolecules* **2007**, *8*, 1824−1829.

(7) Bonincontro, A.; Falivene, M.; La Mesa, C.; Risuleo, G.; Ruiz Peña, M. Dynamics of DNA adsorption on and release from SDS-DDAB catanionic vesicles: A multitechnique study. *Langmuir* **2008**, *24*, 1973−1978.

(8) Colomer, A.; Pinazo, A.; Manresa, M. A.; Vinardell, M. P.; Mitjans, M.; Infante, M. R.; Peréz, L. Cationic surfactants derive from lysine: Effects of their stucture and charge type on antimicrobial and hemolytic activities. *J. Med. Chem.* **2011**, *54*, 989−1002.

(9) Pinazo, A.; Pons, R.; Peréz, L.; Infante, M. R. Amino acids as raw materials for biocompatible surfactants. *Ind. Eng. Chem. Res.* **2011**, *50*, 4805−4817.

(10) Kocer, A. Functional liposomal membranes for triggered release. *Methods Mol. Biol.* **2010**, *605* (Liposomes,Vol. 1), 243−255.

(11) Kostarelos, K.; Emfietzoglou, D.; Tadros, T. F. Light-sensitive fusion between polymer-coated liposomes following physical anchoring of polymerizable polymers onto lipid bi-layers by self-assembly. *Faraday Discuss.* **2004**, *128* (Self-Organising Polymers), 379−388.

(12) Jokela, P.; Jönsson, B.; Khan, A. Phase equilibria of catanionic surfactant-water systems. *J. Phys. Chem.* **1987**, *91*, 3291−3298.

(13) Marques, E. F.; Brito, R. O.; Silva, S. G.; Rodriguez-Borges, J. E.; do Vale, M. L.; Gomes, P.; Araujo, M. J.; Soderman, O. Spontaneous vesicle formation in catanionic mixtures of amino acid-based surfactants: Chain length symmetry effects. *Langmuir* **2008**, *24*, 11009−11017.

(14) Andreozzi, P.; Funari, S. S.; La Mesa, C.; Mariani, P.; Ortore, M. G.; Sinibaldi, R.; Spinozzi, F. Multi- to unilamellar transitions in catanionic vesicles. *J. Phys. Chem. B* **2010**, *114*, 8056−8060.

(15) Manconi, M.; Vila, A. O.; Sinico, C.; Figueruelo, J.; Molina, F.; Fadda, A. M. Theoretical and experimental evaluation of decypolyglucoside vesicles as potential drug delivery systems. *J. Drug Delivery Sci. Technol.* **2006**, *16*, 141−146.

(16) Aiello, C.; Andreozzi, P.; La Mesa, C.; Risuleo, G. Biological activity of SDS-CTAB catanionic vesicles in cultured cells and assessment of their cytotoxicity ending in apoptosis. *Colloids Surf., B* **2010**, *78*, 149−154.
(17) Russo, L.; Berardi, V.; Tardani, F.; La Mesa, C.; Risuleo, G. Delivery of RNA and its intracellular translation into protein mediated by SDS-CTAB vesicles: potential use in nanobiotechnology. *BioMed. Res. Int.* **2013**, *734596*, 1−7.
(18) Marques, E. F. Size and stability of catanionic vesicles: Effects of formation path, sonication, and aging. *Langmuir* **2000**, *16*, 4798−4807.
(19) Caria, A.; Khan, A. Phase behavior of catanionic surfactant mixtures: Sodium bis-(2-ethylhexyl) sulfosuccinate-didodecyldimethylammonium bromide-water system. *Langmuir* **1996**, *12*, 6282−6290.
(20) Barbetta, A.; La Mesa, C.; Muzzi, L.; Pucci, C.; Risuleo, G.; Tardani, F. Catanionic vesicular systems as potential carriers in nanotechnologies. In *Nanobiotechnology*; One Central Press: 2014, in press.
(21) Liu, D. L.; Qiao, W. H.; Li, S. Z.; Chen, Y.; Cui, X.; Li, K.; Yu, L.; Yan, K.; Zhu, L.; Guo, Y.; Cheng, L. B. Structure-function relationship research of glycerol backbone-based cationic lipids for gene delivery. *Chem. Biol. Drug Des.* **2008**, *71*, 336−344.
(22) Pucci, C.; Salvia, A.; Ortore, M. G.; La Mesa, C. The DODAB/AOT/water system: vesicle formation and interactions with salts or synthetic polyelectrolytes. *Soft Matter* **2013**, *9*, 9000−9007.
(23) Marques, E. F.; Regev, O.; Edlund, H.; Khan, A. Micelles, dispersions, and liquid crystals in the catanionic mixture bile salt-double-chained surfactant. The bile salt-rich area. *Langmuir* **2000**, *16*, 8255−8562.
(24) Marques, E. F.; Regev, O.; Khan, A.; Lindman, B. Vesicle formation and general phase behavior in the catanionic mixture SDS-DDAB-water. The cationic-rich side. *J. Phys. Chem. B* **1999**, *103*, 8353−8363.
(25) Marques, E. F.; Regev, O.; Khan, A.; De Graca, M. M.; Lindman, B. Vesicle formation and general phase behavior in the catanionic mixture SDS-DDAB-water. The anionic-rich side. *J. Phys. Chem. B* **1998**, *102*, 6746−6758.
(26) Huang, Z.-L.; Hong, J. Y.; Chang, C.-H.; Yang, Y.-M. Gelation of charged catanionic vesicles prepared by a semispontaneous process. *Langmuir* **2010**, *26*, 2374−2382.
(27) Chang, J.-X.; Wang, H.-Q.; Zhao, G.-Q.; Chu, H.-Y.; Zhang, G.-J. International construction and characterization of a eukaryotic expression vector for small interfering RNA targeting the NEDD9 gene. *J. Mol. Med.* **2012**, *30*, 1343−1348.
(28) Anders, L.; Guenther, M. G.; Qi, J.; Fan, Z. P.; Marineau, J. J.; Rahl, P. B.; Alla, J. L.; Sigova, A.; Smith, W. B.; Lee, T. I.; Bradner, J. E.; Young, R. A. Genome-wide localization of small molecules. *Nat. Biotechnol.* **2013**, DOI: 10.1038/nbt.2776.
(29) La Mesa, C.; Coppola, L.; Ranieri, G. A.; Terenzi, M.; Chidichimo, G. Phase diagram and phase properties of the system water-hexane-aerosol OT. *Langmuir* **1992**, *8*, 2616−2622.
(30) Svitova, T. F.; Smirnova, Y. P.; Pisarev, S. A.; Berezina, N. A. Self-assembly in double-tailed surfactants in dilute aqueous solutions. *Colloids Surf., A* **1995**, *98*, 107−115.
(31) Collinet-Fressancourt, M.; Leclercq, L.; Bauduin, P.; Aubry, J.; Nardello-Rataj, V. Counter anion effect on the self-aggregation of dimethyl-di-N-octylammonium cation: A dual behavior between hydrotropes and surfactants. *J. Phys. Chem. B* **2011**, *115*, 11619−11630.
(32) Daoust, H.; Ferland, P. Solvent-induced conformational change of poly(L-ornithine) and poly(L-lysine) hydrobromides in water-2-chloroethanol mixed solvent. *Eur. Polym. J.* **1989**, *25*, 105−110.
(33) Van de Pas, J. C. Liquid detergents. *Tenside, Surfactants, Deterg.* **1991**, *28*, 158−162.
(34) Rosevear, F. B. The microscopy of the liquid crystalline neat and middle phases of soaps and synthetic detergents. *J. Am. Oil Chem. Soc.* **1954**, *31*, 628−639.
(35) Rosevear, F. B. Liquid crystals: the mesomorphic phases of surfactant compositions. *J. Soc. Cosmet. Chem.* **1968**, *19*, 581−594.
(36) D'Archivio, A. A.; Galantini, L.; Panatta, A.; Tettamanti, E. On the growth and shape of sodium taurodeoxycholate micellar aggregates: A spin-label and quasielastic light scattering investigation. *J. Chem. Phys.* **2004**, *120*, 4800−4807.
(37) Adamson, A. W. *Physical Chemistry of Surfaces*, Vth ed.; Wiley: New York, 1990; Chapter V, pp 218−226.
(38) Hunter, R. J. *Foundations of Colloid Science*; Clarendon Press: Oxford, 1995; Vol. *II*, Chapter 13, pp 807−808.
(39) Pucci, C.; Scipioni, A.; La Mesa, C. Albumin binding onto synthetic vesicles. *Soft Matter* **2012**, *8*, 9669−9675.
(40) Sinibaldi, R.; Ortore, M. G.; Spinozzi, F.; Funari, S.; Teixeira, J.; Mariani, P. SANS/SAXS study of the BSA solvation properties in aqueous urea solutions via a global fit approach. *Eur. Biophys. J.* **2008**, *37*, 673−681.
(41) Moroi, Y. *Micelles. Theoretical and Applied Aspects*; Plenum Press: New York, 1992; Chapter X, pp 183−189.
(42) Muzzalupo, R.; Gente, G.; La Mesa, C.; Caponetti, E.; Chillura-Martino, D.; Pedone, L.; Saladino, M. L. Micelles in mixtures of sodium dodecyl sulfate and a bolaform surfactant. *Langmuir* **2006**, *22*, 6001−6009.
(43) Khan, A.; Marques, E. F. Synergism and polymorphism in mixed surfactant systems. *Curr. Opin. Colloid Interface Sci.* **2000**, *4*, 402−410.
(44) Pucci, C.; Barbetta, A.; Sciscione, F.; Tardani, F.; la Mesa, C. Ion distribution around synthetic vesicles of the catanionic type. *J. Phys. Chem. B* **2014**, *118*, 557−566.
(45) Israelachvili, J. N.; Mitchell, D. J.; Ninham, B. W. Theory of self-assembly of hydrocarbon amphiphiles into micelles and bilayers. *J. Chem. Soc., Faraday Trans. 2* **1976**, *72*, 1525−1568.
(46) Ninham, B. W.; Evans, D. F. The Rideal lecture: Vesicles and molecular forces. *Faraday Discuss. Chem. Soc.* **1986**, *81*, 1−17.
(47) Winsor, P. A. Binary and multicomponent solutions of amphiphilic compounds. Solubilization and the formation, structure, and theoretical significance of liquid crystalline solutions. *Chem. Rev.* **1968**, *68*, 1−40.
(48) Cardini, G.; Baglioni, P.; Taddei, G. Crystalline structures of condensed films at liquid interfaces. *Chem. Phys. Lett.* **1982**, *93*, 533−537.
(49) Ferrer-Tasies, L.; Moreno-Calvo, E.; Cano-Sarabia, M.; Aguilella-Arzo, M.; Angelova, A.; Lesieur, S.; Ricart, S. A.; Faraudo, J.; Ventosa, N.; Veciana, J. Quatsomes: Vesicles formed by self-assembly of sterols and quaternary ammonium surfactants. *Langmuir* **2013**, *29*, 6519−6528.
(50) Jurašin, D.; Vinceković, M.; Pustak, A.; Šmit, I.; Bujan, M.; Filipović-Vinceković, N. Lamellar to hexagonal columnar liquid crystalline phase transition in a catanionic surfactant mixture: dodecylammonium chloride-sodium bis(2-ethylhexyl) sulfosuccinate. *Soft Matter* **2013**, *9*, 3349−3360.
(51) Stanich, C. A.; Honerkamp-Smith, A. R.; Putzel, G. G.; Warth, C. S.; Lamprecht, A. K.; Mandal, P.; Mann, E.; Hua, T.-A. D.; Keller, S. L. Coarsening dynamics of domains in lipid membranes. *Biophys. J.* **2013**, *105*, 444−454.
(52) Letizia, C.; Andreozzi, P.; Scipioni, A.; La Mesa, C.; Bonincontro, A.; Spigone, E. Protein binding onto surfactant-based synthetic vesicles. *J. Phys. Chem. B* **2007**, *111*, 898−908.
(53) Moernstam, B.; Wahlund, K. G.; Joensson, B. Potentiometric acid-base titration of a colloidal solution. *Anal. Chem.* **1997**, *69*, 5037−5044.
(54) Shai, Y. Mechanism of the binding, insertion and destabilization of phospholipid bilayer membranes by α-helical antimicrobial and cell non-selective membrane-lytic peptides. *Biochim. Biophys. Acta* **1999**, *1462*, 55−70.
(55) Bonincontro, A.; Spigone, E.; Pena, M. R.; Letizia, C.; La Mesa, C. Lysozyme binding onto catanionic vesicles. *J. Colloid Interface Sci.* **2006**, *304*, 342−347.
(56) Marques, E. F.; Regev, O.; Khan, A.; Miguel, M. G.; Lindman, B. Interactions between catanionic vesicles and oppositely charged polyelectrolytes: Phase behavior and phase structure. *Macromolecules* **1999**, *32*, 6626−6637.
(57) Ladokhin, A. S.; Selsted, M. E.; White, S. H. Sizing membrane pores in lipid vesicles by leakage of co-encapsulated markers: Pore formation by melittin. *Biophys. J.* **1997**, *72*, 1762−1766.

(58) Ohshima, H. Electrophoretic mobility of soft particles. *J. Colloid Interface Sci.* **1994**, *163*, 474−483.
(59) Ohshima, H.; Nakamura, M.; Kondo, T. Electrophoretic mobility of colloidal particles coated with a layer of adsorbed polymers. *Colloid Polym. Sci.* **1992**, *270*, 873−877.
(60) Ohshima, H. Electrophoretic mobility of soft particles. *Colloids Surf., A* **1995**, *103*, 249−255.
(61) Dobrynin, A. V.; Rubinstein, M.; Joanny, J.-F. Adsorption of a polyampholyte chain on a charged surface. *Macromolecules* **1997**, *30*, 4332−4341.
(62) Dobrynin, A. V.; Obukhov, S. P.; Rubinstein, M. Long-range multichain adsorption of polyampholytes on a charged surface. *Macromolecules* **1999**, *32*, 5689−5700.
(63) Dobrynin, A. V.; Zhulina, E. B.; Rubinstein, M. Structure of adsorbed polyampholyte layers at charged objects. *Macromolecules* **2001**, *34*, 627−639.
(64) Dobrynin, A. V.; Deshkovski, A.; Rubinstein, M. Adsorption of polyelectrolytes at oppositely charged surfaces. *Macromolecules* **2001**, *34*, 3421−3436.
(65) Dobrynin, A. V.; Rubinstein, M. Adsorption of hydrophobic polyelectrolytes at oppositely charged surfaces. *Macromolecules* **2002**, *35*, 2754−2768.